PERFORMANCE BOUNDS ANALYSIS IN MULTICHANNEL DIFFUSION-MRI

Farid AHMED SID[1], *Karim ABED-MERAIM*[2], *Rachid HARBA*[2], *Fatima OULEBSIR-BOUMGHAR*[1]

[1]ParIMéd/LRPE,FEI,USTHB, BP 32 El Alia, Bab Ezzouar, 16111 Algiers, Algeria
[2]PRISME Laboratory, University of Orléans, 12 Rue de Blois, 45067 Orléans, France

ABSTRACT

In this paper, we develop Cramèr-Rao Bound (CRB) expressions in multichannel diffusion MRI. We consider a multi-tensor model with a Non-central Chi (Nc-Chi) distributed noise. The CRB formulas involve integral expressions that are numerically evaluated. In a second step, we propose to simplify the CRB calculation by introducing two analytical approximate expressions for high SNR and low SNR, respectively. Moreover, we develop CRB formulas for the parameters of clinical interest such as the Fractional Anisotropy (FA) and the principal tensor directions. Finally, we exploit these CRBs to analyze the impact of controllable system parameters (e.g. b-value, number of gradient diffusion, number of acquisition coils, etc.) on the clinical parameter estimation in view of future optimal design of the acquisition protocol.

Index Terms— Cramèr-Rao Bound, dMRI, Nc-Chi distribution, multiple coils, multi-tensor model.

1. INTRODUCTION

The diffusion Magnetic Resonance Imaging (dMRI) modality is a unique non invasive technique used, in-vivo, to probe the white matter structure of the brain, in order to get access to the nerve-fiber bundles architecture. The signal attenuation measurements, in each voxel, when a magnetic gradient diffusion field is applied, reflect the Brownian random motion of water molecules. Several methods have already been proposed in the literature to model the observed anisotropic diffusion of water molecules in the brain's white matter. The Diffusion Tensor (DT) model is the most popular one that is used to successfully reconstruct many white matter bundles. Quantities derived from the DT model such as Fractional Anisotropy (FA) and Mean Diffusivity (MD) are widely used to diagnose neurodegenerative diseases like multiple scleroses, Alzheimer, or tumors [1]. This model is, however, valid only for voxels in which there is a single nerve-fiber bundle, and therefore cannot be valid for complex fiber bundles configuration such as crossing or kissing. To overcome this limitation, various techniques have been proposed in the literature including the Multi-Tensor Model (MTM) proposed in [2]. This model, and due to its simplicity, seems to be the best candidate to replace the use of DT model in clinical routine and fiber tracking (Tractography) since it allows the computation of DT for each nerve-fiber bundle independently.

In this paper, we examine the performance bounds related to this model when accounting for the real nature of the noise (which depends on the image reconstruction technique from the different acquisition coils). For this, we adopt the CRB to theoretically determine the optimal estimation precision of the MTM parameters. Previous works that compute the CRB for diffusion MRI models, particularly [3–6], the given FIM expression involve integral formulas that are numerically evaluated, to avoid the integral calculus and to get more tractable FIM expressions, we introduce two analytical approximate expressions for high SNR and low SNR, respectively, Moreover, we develop CRB formulas for the parameters of clinical interest such as the Fractional Anisotropy (FA) and the principal tensor directions. In particular, the CRB derivation allows us to analyze the dependency of the estimation accuracy on tunable acquisition protocol parameters (b-value, number of gradient diffusion, number of acquisition coils, etc.) in view of future optimal design of the system.

2. SIGNAL AND NOISE MODEL

For simplicity, we consider here the bi-tensor[1] model. For any given voxel the signal intensity in the noiseless case is,

$$A_{k,j} = S_0(fe^{-b_j \mathbf{g}_{k,j}^T \mathbf{D}_1 \mathbf{g}_{k,j}} + (1-f)e^{-b_j \mathbf{g}_{k,j}^T \mathbf{D}_2 \mathbf{g}_{k,j}}), \quad (1)$$

where b_j is the j^{th} diffusion-weighting coefficient known as b-value, $j = 1, \cdots, J$. J is the number of shell (b-value) used for the acquisition of dMRI data, and $\mathbf{g}_{k,j}$ is a unit vector representing the k^{th} gradient direction, $k = 1, \cdots, K_j$ (we assume that K_j gradient directions are associated with the j^{th} b-value b_j according to [7], see Figure 1). f and $(1-f)$ are the fractions of occupancy of the fiber bundles. S_0 is the known signal intensity when $b = 0$. $\mathbf{D}_1$ and $\mathbf{D}_2$ are the diffusion tensors symmetric matrices associated with the two fiber bundles.

With the hardware currently provided by the major vendors and equipped by multiple acquisition coils, the signal intensity measured in the l^{th} coil when the k^{th} direction of the diffusion gradient field is applied and for a b-value b_j, can

[1]The extension to a larger number of tensors is straightforward but tedious.

978-0-9928626-3-3/15/$31.00 ©2015 IEEE

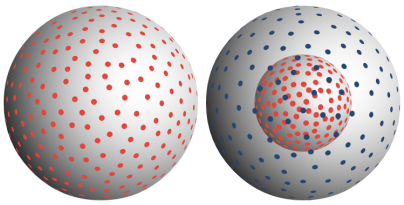

Fig. 1. The encoded diffusion gradient directions as vertices of a tessellated sphere: On the left, single-shell, j=1, dMRI data are acquired with one b-value and one set of gradient (e.g. 1000 $s.mm^{-2} \times 60$ $directions$). On the right, double shell, j=2, two b-value associated with two set of gradient directions (e.g. 1000 $s.mm^{-2} \times 30$ $directions$ and 1500 $s.mm^{-2} \times 30$ $directions$) [7].

be expressed as $S_{klj} = c_l A_{k,j} + \mathcal{N}_{klj}(0, \sigma^2)$, where c_l is the sensitivity of the l^{th} coil at the voxel under consideration and $\mathcal{N}_{klj}(0, \sigma^2)$ an additive white Gaussian noise process with zero-mean and variance σ^2. Hence, the intensity of any voxel in the reconstructed image with a sum-of-squares (SoS) technique [8], follows the Nc-Chi distribution defined by:

$$\mathcal{P}(S_{kj}, A_{kj}, L, \sigma) = \frac{A_{kj}^{1-L} S_{kj}^{L}}{\sigma^2} e^{-\frac{S_{kj}^2 + A_{kj}^2}{2\sigma^2}} I_{L-1}(\frac{A_{kj} S_{kj}}{\sigma^2}), \quad (2)$$

where $I_{L-1}(.)$ is the modified $(L-1)^{th}$ order Bessel function of the first kind, L is the number of acquisition coils, S_{kj} is the reconstructed image voxel intensity (i.e. $S_{kj} = (\sum_l S_{klj}^2)^{1/2}$) and A_{kj} is the total image voxel intensity in the absence of noise, taking into account the contribution of all the coils, given by:

$$A_{kj} = C_L S_0 (f e^{-b_j \mathbf{g}_{kj}^T \mathbf{D}_1 \mathbf{g}_{kj}} + (1-f) e^{-b_j \mathbf{g}_{kj}^T \mathbf{D}_2 \mathbf{g}_{kj}}), \quad (3)$$

where $C_L = (\sum_{l=1}^{L} c_l^2)^{\frac{1}{2}}$ is the sensitivity factor assumed known.

3. CRAMER-RAO LOWER BOUND

3.1. Theory

Cramer-Rao lower bounds provide fundamental limits to the accuracy with which a parameter can be determined from any experimental data using unbiased estimation methods. Indeed, for a given statistical model depending on a parameter vector $\mathbf{\Theta}$, the mean square error of any unbiased estimator of $\mathbf{\Theta}$ is lower bounded by the CRB computed as the inverse of the Fisher Information Matrix (FIM). The parameters vector in our case is $\mathbf{\Theta} = [\mathbf{d}_1^T, \mathbf{d}_2^T, f, \sigma]^T$ ($\mathbf{d}_i = [d_1^{(i)}, \ldots, d_6^{(i)}]^T$ is the six-element vector rearrangement of $\mathbf{D}_i$, i=1,2) to be estimated from the observed (noisy) data vector $\mathbf{S} = [\mathbf{S}_1^T, \cdots, \mathbf{S}_J^T]^T$ (where $\mathbf{S}_j$ represents the set of K_j measurements for the b-value b_j). The likelihood function is denoted by $L(S, \Theta)$ and the total number of measurements is $K = K_1 + \cdots + K_J$. The $(i,j)^{th}$ entry of the FIM matrix is given by [9]: $\mathbf{F}_{i,j}(\Theta) = -\mathbb{E}[(\frac{\partial^2 \ln(L(S,\Theta))}{\partial\theta_i \partial\theta_j})]$ where $\mathbb{E}[.]$ stands for the statistical expectation operator. If $\hat{\zeta}$ represents an unbiased estimator of $\zeta(\Theta)$ a function of Θ, then, its error covariance matrix is larger or equal to the CRB, i.e.:

$$Cov(\zeta) \geq \bigtriangledown\zeta(\Theta) CRB(\Theta) (\bigtriangledown\zeta(\Theta))^T, \quad (4)$$

with $CRB(\Theta) = \mathbf{F}^{-1}(\Theta)$ and $\bigtriangledown\zeta(\Theta)$ is the gradient matrix which $(i,j)^{th}$ entry is $\dfrac{\partial\zeta_i}{\partial\theta_j}$.

3.2. Exact CRB

Since the K Diffusion MRI measurements, are statistically independent, the likelihood function can be written as:

$$L(S, \Theta) = \prod_{k,j} \mathcal{P}(S_{kj}, A_{kj}, L, \sigma). \quad (5)$$

and hence the log-likelihood function is

$$\mathcal{L}(\Theta) = \ln L(S, \Theta) = \sum_{k,j} \{-2\ln(\sigma) + (1-L)\ln(A_{kj}) + L\ln(S_{kj}) - \frac{A_{kj}^2 + S_{kj}^2}{2\sigma^2} + \ln I_{L-1}(x_{kj})\} \quad (6)$$

with $x_{kj} = \frac{A_{kj} S_{kj}}{\sigma^2}$. Using general derivation properties and recurrence relation of the Bessel function [10], we obtain:

$$\frac{\partial\mathcal{L}(\Theta)}{\partial\theta_i} = \frac{1}{\sigma^2} \sum_{k,j} \{(S_{kj} \frac{I_L(x_{kj})}{I_{L-1}(x_{kj})} - A_{kj}) \frac{\partial A_{kj}}{\partial\theta_i}\}, \ \theta_i \neq \sigma$$

$$\frac{\partial\mathcal{L}(\Theta)}{\partial\theta_i} = \sum_{k,j} \{\frac{S_{kj}^2 + A_{kj}^2}{\sigma^3} - \frac{2 S_{kj} A_{kj}}{\sigma^3} \frac{I_L(x_{kj})}{I_{L-1}(x_{kj})} - \frac{2L}{\sigma}\}, \theta_i = \sigma$$

After some tedious but straightforward derivations, we get the elements of the FIM:

$$F_{m,n} = \sum_{k,j} [\frac{1}{\sigma^2} \frac{\partial A_{kj}}{\partial\theta_m} \frac{\partial A_{kj}}{\partial\theta_n} \mathcal{M}_{kj}], \ 1 \leq m, n \leq 13. \quad (7)$$

$$F_{m,14} = -\frac{2}{\sigma^2} \sum_{k,j} [\eta_{kj} \frac{\partial A_{kj}}{\partial\theta_m} (\mathcal{M}_{kj} - 1)], \quad 1 \leq m \leq 13 \quad (8)$$

$$F_{14,14} = \sum_{k,j} \frac{4}{\sigma^2} [L - \eta_{kj}^2 (\mathcal{M}_{kj} - 1)], \ (\theta_m = \theta_n = \sigma) \quad (9)$$

with:

$$\mathcal{M}_{kj} = \mathbb{E}[\frac{x_{kj}^2}{\eta_{kj}^2} \frac{I_L^2(x_{kj})}{I_{L-1}^2(x_{kj})}] - \eta_{kj}^2, \quad (10)$$

$\eta_{kj} = \frac{A_{kj}}{\sigma}$. Using (2), $\mathcal{M}_{kj}$ is computed as:

$$\mathcal{M}_{kj} = \eta_{kj}^{-2(L+1)} e^{-\frac{\eta_{kj}^2}{2}} \int_0^{+\infty} x^{L+2} e^{-\frac{x^2}{2\eta_{kj}^2}} \frac{I_L^2(x)}{I_{L-1}(x)} dx - \eta_{kj}^2 \quad (11)$$

Unfortunately, the integral in (11) does not admit a closed form expression, hence it is evaluated numerically. Using MATLAB, the Bessel function $I_L(x)$ is available under the

command $besseli(L,x)$. However direct usage of this function will be prone to numerical errors, due to the large dynamical range of Bessel function values. Fortunately, there is a scaled version of Bessel function in MATLAB under the command $besseli(L,x,1)$ equal to $\check{I}_L(x) = I_L(x)e^{-x}$ which solves this numerical problem according to:

$$\mathcal{M}_{kj} = \eta_{kj}^{-2(L+1)} e^{-\frac{\eta_{kj}^2}{2}} \int_0^{+\infty} x^{L+2} e^{x-\frac{x^2}{2\eta_{kj}^2}} \frac{\check{I}_L^2(x)}{\check{I}_{L-1}(x)} dx - \eta_{kj}^2. \quad (12)$$

In matrix form, the FIM can be written as: $\mathbf{F} = \sum_{j=1}^{J} \mathbf{F}_j$, where $\mathbf{F}_j$ is a symmetric matrix with an upper triangular part given by:

$$\begin{pmatrix} \boldsymbol{G}_j\boldsymbol{\Lambda}_{1j}\boldsymbol{G}_j^T & \boldsymbol{G}_j\boldsymbol{\Lambda}_{3j}\boldsymbol{G}_j^T & \boldsymbol{G}_j\boldsymbol{\Lambda}_{4j}\boldsymbol{\eta}_j & \frac{2}{\sigma}\boldsymbol{G}_j\boldsymbol{\Lambda}_{5j}\boldsymbol{\eta}_j \\ & \boldsymbol{G}_j\boldsymbol{\Lambda}_{2j}\boldsymbol{G}_j^T & \boldsymbol{G}_j\boldsymbol{\Lambda}_{6j}\boldsymbol{\eta}_j & \frac{2}{\sigma}\boldsymbol{G}_j\boldsymbol{\Lambda}_{7j}\boldsymbol{\eta}_j \\ & & \boldsymbol{\eta}_j^T\boldsymbol{\Lambda}_j\boldsymbol{\eta}_j & \frac{2}{\sigma}\boldsymbol{\eta}_j^T(\boldsymbol{I}-\boldsymbol{\Lambda}_j)\boldsymbol{\eta}_j \\ & & & \frac{4}{\sigma^2}(K_jL - \boldsymbol{\eta}_j^T(\boldsymbol{I}-\boldsymbol{\Lambda}_j)\boldsymbol{\eta}_j) \end{pmatrix}$$

The $6 \times K_j$ matrix $\mathbf{G}_j$ built from the gradient directions associated to b_j is given by $\mathbf{G}_j = b_j[\tilde{\mathbf{g}}_{1j}, \cdots, \tilde{\mathbf{g}}_{K_jj}]$ where $\tilde{\mathbf{g}}$ satisfies $\mathbf{g}^T\mathbf{D}_1\mathbf{g} = \tilde{\mathbf{g}}^T\mathbf{d}_1$, i.e. if $\mathbf{g} = [g_x, g_y, g_z]^T$ then $\tilde{\mathbf{g}} = [g_x^2, g_y^2, g_z^2, 2g_xg_y, 2g_xg_z, 2g_yg_z]^T$. $\boldsymbol{\eta}_j$ is the SNR vector, whose elements are $\eta_{kj},\ k = 1, \cdots, K_j$. $\boldsymbol{\Lambda}_j, \boldsymbol{\Lambda}_{1j}, \cdots, \boldsymbol{\Lambda}_{7j}$ are $K_j \times K_j$ diagonal matrices, given by:

$\boldsymbol{\Lambda}_{1j} = \boldsymbol{\Lambda}_j diag(\boldsymbol{\eta}_j^1 .* \boldsymbol{\eta}_j^1),\ \boldsymbol{\Lambda}_{2j} = \boldsymbol{\Lambda}_j diag(\boldsymbol{\eta}_j^2 .* \boldsymbol{\eta}_j^2)$
$\boldsymbol{\Lambda}_{3j} = \boldsymbol{\Lambda}_j diag(\boldsymbol{\eta}^1 .* \boldsymbol{\eta}^2),\ \boldsymbol{\Lambda}_{4j} = diag(\boldsymbol{\eta}_j^1)\boldsymbol{\Lambda}_j$
$\boldsymbol{\Lambda}_{5j} = diag(\boldsymbol{\eta}_j^1)(\mathbf{I}-\boldsymbol{\Lambda}_j),\ \boldsymbol{\Lambda}_{6j} = diag(\boldsymbol{\eta}_j^2)\boldsymbol{\Lambda}_j$
$\boldsymbol{\Lambda}_{7j} = diag(\boldsymbol{\eta}_j^2)(\mathbf{I}-\boldsymbol{\Lambda}_j),\ \boldsymbol{\Lambda}_j = diag(\mathcal{M}_{1j}, \cdots, \mathcal{M}_{K_jj})$

where $.*$ denotes the element-wise product, $\mathbf{I}$ the identity matrix and $\boldsymbol{\eta}_j^1$ (resp. $\boldsymbol{\eta}_j^2$) is the K_j dimensional vector which entries are $\frac{fS_0}{\sigma}e^{-b_j\mathbf{g}_{kj}^T\mathbf{D}_1\mathbf{g}_{kj}}$ (resp. $\frac{(1-f)S_0}{\sigma}e^{-b_j\mathbf{g}_{kj}^T\mathbf{D}_2\mathbf{g}_{kj}}$).
As we can see, the FIM elements depend on the SNRs, b-values, number of acquisition coils and the gradient direction field. In the sequel, we will study the effect of these parameters on the CRB and hence on the estimation of the bi-tensor model and its derived quantities.

3.3. Approximate analytical CRB

To avoid the previous integral calculus and to get more tractable FIM expressions, we introduce here some approximations of the fraction $\frac{I_L^2(x)}{I_{L-1}^2(x)}$ which lead to simple and interpretable formulas. These approximations are based on asymptotic Bessel function expansions considered for the high and low SNR cases.

High SNR case: We assume here that η_{kj} is high for all k, j, and use the approximation of the modified Bessel function of the first kind given in [10], for large x values:

$$I_L(x) \sim \frac{e^x}{\sqrt{2\pi x}}\{1 - \frac{4L^2-1}{8x} + \frac{(4L^2-1)(4L^2-9)}{2!(8x)^2} + ...\},$$

which allows us to calculate an asymptotic expansion of $\frac{I_L^2(x)}{I_{L-1}^2(x)}$ as:

$$\frac{I_L^2(x)}{I_{L-1}^2(x)} = 1 - \frac{2L-1}{x} + \frac{(2L-1)(L-1)}{x^2} + O(\frac{1}{x^3}), \quad (13)$$

Plugging (13) in (10) and using the first and second order moments of the Nc-Chi distribution leads to:

$$\mathcal{M}_{kj} \approx 2L + \frac{(2L-1)(L-1)}{\eta_{kj}^2} - \frac{2L-1}{\eta_{kj}}\sqrt{\frac{\pi}{2}}L_{\frac{1}{2}}^{L-1}(-\frac{\eta_{kj}^2}{2}), \quad (14)$$

where $L_{\frac{1}{2}}^{L-1}$ is the generalized Laguerre polynomial.

Low SNR case: in that case we use the following approximation in the vicinity of zero [10]:

$$I_L(x) \sim \frac{(\frac{1}{2}x)^L}{\Gamma(L+1)}, \quad (15)$$

which allows to approximate the fraction $\frac{I_L^2(x)}{I_{L-1}^2(x)}$ as:

$$\frac{I_L^2(x)}{I_{L-1}^2(x)} \approx \frac{1}{4L^2}x^2 \quad (16)$$

Plugging (16) in (10) and using the forth order moments of the Nc-Chi distribution we obtain finally:

$$\mathcal{M}_{kj} = \frac{\eta_{kj}^2}{4L^2}[3\eta_{kj}^2 + (\eta_{kj}^2+1)(\eta_{kj}^2+4L)]. \quad (17)$$

In Figure 2, we plot the exact CRB and our approximate analytical CRB for both high and low SNR cases. The ordinate show the optimal estimation error (square root of the CRB) of the largest eigenvalue of a typical tensor as a function of the number of gradient directions. Since the SNR cannot be set by the user, for simulation, the largest (resp. the lowest) attenuated diffusion signal direction was chosen to keep the SNR in the high SNR (resp. low SNR) range. Our simulation results show that these analytical formulas provide very good approximations of the FIM and hence the CRB expressions.

3.4. CRB of clinical interest parameters

The Diffusion Tensors $\mathbf{D}_1$ and $\mathbf{D}_2$ are 3×3 symmetric and positive-definite matrices that describe the water molecule diffusion process through their spectral elements, i.e. their eigenvalues and eigenvectors denoted $\lambda_1^i, \lambda_2^i, \lambda_3^i$ and $\mathbf{V}^i = [\mathbf{v}_1^i, \mathbf{v}_2^i, \mathbf{v}_3^i]$, $i = 1, 2$ respectively. In clinical application, the FA is the index used to measure the anisotropy of the brain tissues. It is calculated as :

$$FA^i = \sqrt{\frac{(\lambda_1^i - \lambda_2^i)^2 + (\lambda_1^i - \lambda_3^i)^2 + (\lambda_2^i - \lambda_3^i)^2}{2((\lambda_1^i)^2 + (\lambda_2^i)^2 + (\lambda_3^i)^2)}} \quad (18)$$

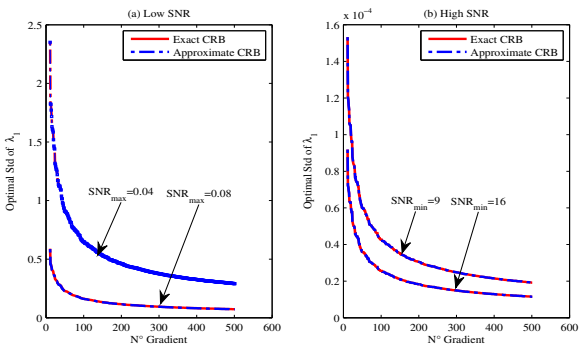

Fig. 2. Comparison between Exact CRB and our approximate analytical CRB.

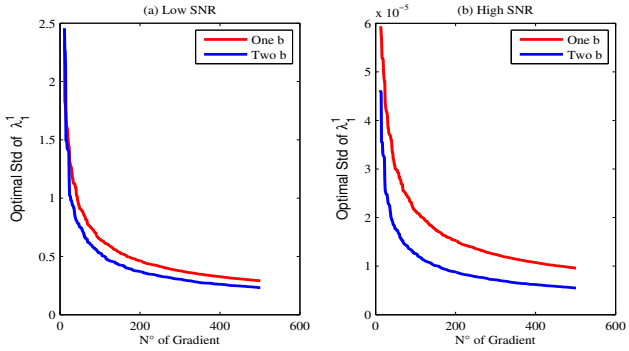

Fig. 3. Influence of the number of gradient directions on λ_1^1.

Using (4), the estimation of this clinical parameter is lower bounded (in terms of mean squares error) by:

$$CRB(FA^i) = \nabla_{(FA^i)} CRB(\lambda^i) \nabla_{(FA^i)^T}, \qquad (19)$$

where $\nabla_{(FA^i)}$ is the gradient vector given by $[\frac{\partial FA^i}{\partial \lambda_1^i}, \frac{\partial FA^i}{\partial \lambda_2^i}, \frac{\partial FA^i}{\partial \lambda_3^i}]$, and $CRB(\lambda^i)$ is the CRB for the eigenvalues of the i^{th} tensor given by:

$$CRB(\lambda^i) = \nabla(\lambda)\, CRB(D_i)\, \nabla(\lambda)^T \qquad (20)$$

where $CRB(D_i)$ denotes the CRB for the i^{th} tensor parameters given by the i^{th} 6×6 diagonal bloc of the CRB matrix computed previously. $\nabla(\lambda)$ denotes the 3×6 gradient matrix given by [11]:

$$\nabla(\lambda) = (\mathbf{V}^i \odot \mathbf{V}^i)^T \mathbf{J} \qquad (21)$$

$\odot$ being the Khatri-Rao product and $\mathbf{J}$ is a selection matrix defined by $vec(\mathbf{D}_i) = \mathbf{J}\mathbf{d}_i$.
Due to lack of space in the paper, the CRBs of the principal tensor directions (used in the tractography) will be presented and thoroughly analyzed in an extended version of this work.

4. PERFORMANCE BOUNDS ANALYSIS

In this section we exploit the developed CRBs to analyze the impact of controllable system parameters (e.g. b-value, number of gradient diffusion, and number of acquisition coils) on the estimation of the bi-tensor parameters. We present here the optimal standard deviation (Std) computed as the square root of the CRB for the largest eigenvalue λ_1^1 and Fractional Anisotropy FA^1 of the first tensor (similar results have been observed for tensor 2). We simulate fiber crossing by generating diffusion MRI data with representative diffusion values, selected from a very anisotropic voxel of the human white matter, from the body of the corpus callosum [12].
$[\lambda_1^1, \lambda_2^1, \lambda_3^1] = [1708, 303, 114] \times 10^{-6} mm^2.s^{-1}$,
$[\lambda_1^2, \lambda_2^2, \lambda_3^2] = [1685, 287, 109] \times 10^{-6} mm^2.s^{-1}$.
We have used 500 diffusion encoding gradient directions distributed on the unit sphere according to [7]. In the case of the single-shell, there is insufficient data to resolve the degrees of freedom of both volume fractions and tensors respectively. So instead of using the model in (1) we use direct sum of the two exponentials because the volume fractions f and $(1-f)$ can be integrated into the diffusion tensors D_1 and D_2 respectively.
$fe^{-b\mathbf{g}^T \check{\mathbf{D}}_1 \mathbf{g}} = e^{-b\mathbf{g}^T(\check{\mathbf{D}}_1 - \frac{\ln(f)}{b}\mathbf{I})\mathbf{g}} = e^{-b\mathbf{g}^T \mathbf{D}_1 \mathbf{g}}$.
We considered $b = 1000\, s.mm^{-2}$ for the single-shell case and $b_1 = 1000\, s.mm^{-2}$, $b_2 = 1500\, s.mm^{-2}$ for the multi-shell case.

4.1. Effect of the number of diffusion gradient directions

In Figure 3, we show the minimum estimation error of the largest eigenvalue λ_1^1 as a function of the number of gradients, assuming $L = 1$. It can be seen that better accuracy in the estimation of the largest eigenvalue can be obtained by including more diffusion gradient directions. One can see, however, that with about 100 to 200 gradient directions one is very close to the performance obtained with 500 directions. Indeed, we observes a large gain when varying the number of gradients in the range $[14 - 100]$ after which the gain becomes less and less significant. Finally, for high SNR case, we can notice that using two b-values improves significantly the estimation accuracy. For example, from Figure 3-b, we can see that working with two b-values and about 100 gradient directions is as good as working with a single b value and 500 gradient directions (the latter being much more costly in terms of acquisition time).

4.2. Effect of the number of coils

For multi-channel systems, the image reconstruction technique combines information from different acquisition coils. To examine the effect of increasing the number of coils in the estimation of the bi-tensor model parameters, we have fixed the number of diffusion gradient directions to 60. In Figure 4, we show the estimation error of the largest eigenvalue λ_1^1 as a function of the number of acquisition coils for low and high SNR cases. We note that continue to increasing the number

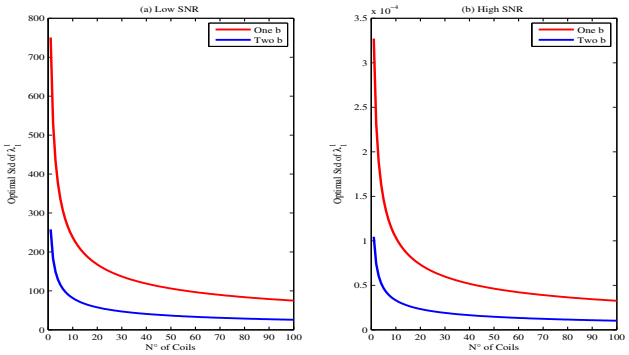

Fig. 4. Influence of the number of acquisition coils on λ_1^1.

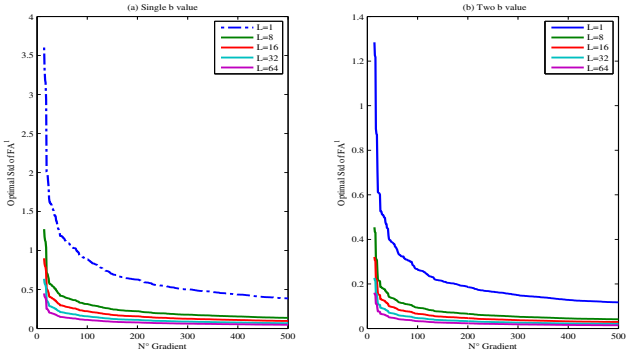

Fig. 5. Influence of the number of gradient directions, b value and the number of acquisition coils on the FA.

of coils does not improve significantly the accuracy because the CRB will decrease $\sqrt{L}$ times with respect to a single-coil system. Working with two b values, improves significantly the performance accuracy.

4.3. Impact of multiple-coil systems and the diffusion gradient directions on FA

In Figure 5, we show simulated results that illustrate the estimate error of FA^1 as a function of the number of gradient directions, in the case of single b value and two b values, for different number of acquisition coils. The obtained results confirm our previous results discussed in sections 4.1 and 4.2. The estimation gain is obvious when considering two shells (Figure 5-b).

5. CONCLUSION

In this paper, we have developed Cramèr-Rao Bound (CRB) expressions in multichannel diffusion MRI. We have considered a multi-tensor model with a non-central Chi distributed noise. These CRBs represent a powerful theoretical tool to analyze the performance of such system and to optimize the tuning of its parameters. Due to space limitation, we have restricted our study to the impact of the number of diffusion gradient directions, the number of acquisition coils, the SNR and the b value on the estimation of the largest eigenvalue and the FA of the first tensor. These preliminary results show that to reduce the scan time while preserving a good estimation accuracy, it is preferable to increase the number of acquisition coils rather than the number of gradient directions and to prefer working with multiple shells.

REFERENCES

[1] Horsfield MA, Jones DK, "Applications of diffusion-weighted and diffusion tensor MRI to white matter diseases-a review," *NMR Bio.*, pp. 15(7–8):570–7, 2002.

[2] Tuch, DS., *Diffusion MRI of Complex Tissue Structure*, Ph.D. thesis, MIT, 2002.

[3] Alexander DC, " A general framework for experiment design in diffusion MRI and its application in measuring direct tissue-microstructure features," *Magn Reson Med*, pp. 60(2):439–48, 2008.

[4] Beltrachini L, von Ellenrieder N, Muravchik CH, " Error bounds in diffusion tensor estimation using multiple-coil acquisition systems," *Magn Reson Med*, pp. 31(8):1372–83, 2013.

[5] Caan MW, Khedoe HG, Poot DH, den Dekker AJ, Olabarriaga SD, Grimbergen KA, van Vliet LJ, Vos FM, "Estimation of diffusion properties in crossing fiber bundles," *IEEE Trans Med Imaging*, pp. 29(8):1504–15, 2010.

[6] Andersson JL, "Maximum a posteriori estimation of diffusion tensor parameters using a Rician noise model: why, how and but," *Neuroimage*, pp. 42(4):1340–56, 2008.

[7] Caruyer E, Lenglet Ch, Sapiro G, Deriche R, "Design of multishell sampling schemes with uniform coverage in diffusion MRI," *Magnetic Res. in Medicine*, vol. 69, no. 6, pp. 1534–1540, 2013.

[8] Dietrich O, Raya JG, Reeder SB, Ingrisch M, Reiser MF, Schoenberg SO, "Influence of multichannel combination, parallel imaging and other reconstruction techniques on MRI noise characteristics," *Magn Reson Med*, pp. 26(6):754–62, 2008.

[9] Steven M. Kay, *Fundamentals of statistical signal processing: estimation theory*, Prentice-Hall: USA, 1993.

[10] Abramowitz M, Stegun IA, *Handbook of mathematical functions*, New York: Dover Publications, 1970.

[11] J. H. Wilkinson, *The algebraic eigenvalue problem*, Oxford Univ. Press, 1965.

[12] Pierpaoli C, Jezzard P, Basser PJ, Barnett A, Di Chiro G., "Diffusion tensor MR imaging of the human brain," *Radiology*, pp. 201(3):637–48, 1996.